Research Article GU J Sci, Part A, 9(4): 452-460 (2022) https://doi.org/10.54287/gujsa.1185023

Gazi University
Journal of Science
PART A: ENGINEERING AND INNOVATION
http://dergipark.org.tr/gujsa

Comparison of Electronic and Magnetic Properties of 4d Transition Metals Based $NbAl_2F_4$ and $TcAl_2F_4$ Spinels

Evren Görkem ÖZDEMİR[1*]

[1]*Gazi University, Faculty of Science, Department of Physics, 06560 Teknikokullar Ankara, Türkiye*

Keywords

Spinel
$NbAl_2F_4$
GGA+mBJ
Half-metallic
$TcAl_2F_4$

Abstract

Half-metallic properties of $NbAl_2F_4$ spinel and semiconductor characteristics of $TcAl_2F_4$ spinel were investigated with the help of the WIEN2k program. $NbAl_2F_4$ spinel shows a metallic character in the up-electron states, while it has a semiconductor nature in the down-electron states. In $NbAl_2F_4$ spinel, the E_g bandgaps were calculated in GGA and GGA+mBJ 1.551 eV and 1.622 eV, respectively. The E_{HM} half-metallic bandgaps were obtained 0.410 eV and 0.422 eV, respectively. In the up-spin states of $TcAl_2F_4$ spinel, E_g values were obtained 1.199 eV and 1.447 eV for the GGA and GGA+mBJ methods, respectively, while they were obtained 1.281 eV and 1.519 eV in the down-spin states, respectively. When GGA+mBJ is used, it is easily observed that the semiconductor characters increase. Total magnetic moments of $NbAl_2F_4$ and $TcAl_2F_4$ spinels were calculated 6.00 μ_B/cell and 10.0 μ_B/cell, respectively. When both electronic and magnetic moment values are carefully examined, $NbAl_2F_4$ and $TcAl_2F_4$ spinels can be used as alternative compounds in spintronic applications.

Cite

Özdemir, E. G. (2022). Comparison of Electronic and Magnetic Properties of 4d Transition Metals Based NbAl2F4 and TcAl2F4 Spinels. *GU J Sci, Part A, 9*(4), 452-460.

Author ID (ORCID Number)

E. G. Özdemir, 0000-0001-9794-1381

Article Process

Submission Date 06.10.2022
Revision Date 31.10.2022
Accepted Date 09.11.2022
Published Date 31.12.2022

1. INTRODUCTION

In recent years, the characteristics of magnetic materials, especially with the effect of their spin orientation, have begun to be used in many areas of technological applications. This branch of science, which forms the basis of spin orientations, is called spintronics. In short, spintronics is the science that examines the technological properties of nano-sized devices depending on their spin orientation. Hirohata et al. (2020) have recently carried out a very detailed study involving spintronic applications. They showed similar and different properties of magnetic and semiconductor devices. Since spin generation and spin-polarized electrons form the basis of spintronic applications, they mentioned the methods by which spins can be polarized even in non-magnetic materials. These methods are spin injection from a magnetic field, an electric field or a ferromagnetic material. Magnetic random-access memories (MRAM) are one of the application products of spintronic technology. Shin et al. (2006) investigated the effects of Cl_2 and O_2 gases with varying density on the Co_2MnSi magnetic film, which was thought to be used for MRAM devices. They experimentally proved that the etch rate of the Co_2MnSi magnetic film decreased with increasing Cl_2 and O_2 gas densities. Quiroz et al. (2020) investigated the properties of Co/TiO_2 bilayer and TiO_2:Co thin films. It was observed that these materials, obtained experimentally at 293 K and 473 K temperatures, had low energy consumption and expanding storage capacities in the applied magnetic field. Just like MRAM, magnetic sensors (MS) are one of the products obtained as a result of spintronic applications. Zhang et al. (2020) investigated the magnetic sensor properties of boron-doped FeGa film. As a result of their experimental measurements, the magnetic sensitivity of the FeGaB magnetic sensor was obtained as 152.1 Hz/mT. This value was found to be almost four times the FeGa film obtained without boron doping. The sensitivity characteristics of the $BaTiO_3$-Fe-Ga&PDMS magnetic

*Corresponding Author, e-mail: evrengorkemozdemir@gazi.edu.tr

sensor were reported by Xu et al. (2022). The best value of the sensitivity of the magnetic sensor was experimentally obtained as 3.4 V/T when the $BaTiO_3$ concentration was 20%. In addition, experimental investigations of silicon-based Bi_2FeNiO_6 double perovskite-based and $MgAl_2O_4$ barrier magnetic tunnel junctions (MTJ) were performed by Ravi (2020) and Khanal et al. (2022), respectively. When Bi_2FeNiO_6 double perovskite was used, tunnelling magnetoresistance varying from 0.2% to 1.8% was obtained at different temperatures. While the magnetic anisotropy energy density of the $MgAl_2O_4$ barrier magnetic tunnel joint annealed at 400 ^{0}C degree was obtained as 2.25 mJ/m^2, 60% success was achieved in the magnetoresistance. As can be seen from the examples, there are many technological devices that spintronic applications are transformed into.

When de Groot et al. (1983) discovered the half-metallic (HM) features of NiMnSb ferromagnetic material, half-metallic materials have also been widely used in spintronic applications. Half-metallic materials attract attention with their 100% spin polarization and different electronic properties under magnetic fields. One of the spin orientations of HM materials shows metallic character around the Fermi energy level, while the other shows semiconductor character. The spin orientation, which shows semiconductor character, adds 100% spin polarization to the materials. Therefore, these materials are true half-metallic. In cases where the Fermi energy level is cut by electrons and still has a band gap, the spin polarization ratio decreases. In such cases, materials are called nearly half-metallic. Birsan and Kuncser (2022) and Patel et al. (2022) investigated the half-metallic character of Zr_2CrAl and Mn_2SiRh Heusler compounds. The HM band gap (E_{HM}) and total magnetic moment of Zr_2CrAl ferrimagnetic compound were calculated as 0.35 eV and 1.00 μ_B/f.u., respectively. In Mn_2SiRh compound, the E_{HM} value was obtained as 0.36 eV. The half-metallic characters of the $Cd_{1-x}Zn_xCr_2Se_4$, $GeGa_2O_4$ and $MnTi_2O_4$ spinels were studied by Bouhbou et al. (2019), Rafiq et al. (2022) and Nadeem et al. (2022), respectively. Differences in half-metallic band gaps were observed according to varying x-amounts of $Cd_{1-x}Zn_xCr_2Se_4$ (x = 0, 0.125, 0.375 and 0.5) compounds. In x=0, the theoretical band gap values were obtained as 0.43 eV and 1.11 eV by GGA and GGA+mBJ methods, respectively. Here, an experimental band gap of 1.3 eV was obtained and the closest theoretical calculation to this value was with GGA+mBJ. It was observed that the theoretical band gaps obtained with increasing x values decreased. $GeGa_2O_4$ oxide spinel showed semiconductor character with band gaps of 1.605 eV in the spin-up state and 1.578 eV in the spin-down state. The $MnTi_2O_{4-x}$ compound was obtained with a direct band gap of about 5 eV in the spin-up states. Here x represents the vanadium concentration. The band gap rises above 5 eV when the compound is changed to $MnTi_{2-x}O_4$. As can be seen from the examples given, spintronic application areas involved different types of materials. One of the most widely used among these types is half-metallic characters. The main purpose of this study is to examine in detail the electronic, magnetic and HM characters of 4d-transition metal-based $NbAl_2F_4$ and $TcAl_2F_4$ spinels. The magnetic moments of $NbAl_2F_4$ and $TcAl_2F_4$ spinels were calculated as 6.00 μ_B/cell and 10.0 μ_B/cell, respectively. $NbAl_2F_4$ spinel has a half-metallic ferromagnetic structure while $TcAl_2F_4$ spinel has a semiconductor nature. Therefore, two different compounds $NbAl_2F_4$ and $TcAl_2F_4$ spinels will be alternative compounds for spintronics applications.

2. MATERIAL AND METHOD

Electronic and magnetic properties of $NbAl_2F_4$ and $TcAl_2F_4$ spinels were performed using WIEN2k developed by Blaha et al. (2020, 2022). Both GGA-PBE (Perdew et al., 1996) and GGA+mBJ (Tran & Blaha, 2009) methods were used with the help of WIEN2k, which is based on Density Functional Theory. Some research on Density Functional Theory and its methods was carried out by Singh (1994). While forming $NbAl_2F_4$ and $TcAl_2F_4$ spinels, 227-space number and Fd-3m symmetry group were chosen.

Here, the transition metals (Nb, Tc), Al and F atoms are placed at the space coordinates of 0.125/0.125/0.125, 0.50/0.50/0.50 and 0.25/0.25/0.25, respectively. The cubic structures obtained with the help of all these space numbers, symmetry groups and atomic coordinates were given in Figure 1. For the initial state calculations, the spin cutoff values ($R_{MT}K_{max}$) were set to 7 giving the minimum energy values. While performing the potential calculations of the atoms using the GGA method, all atoms of the formed structure are examined separately. Therefore, potential calculations of Nb, Tc, Al, and F atoms examined in this study are performed in Muffin-Tin spheres, an imaginary sphere surrounding these atoms. The radii of these Muffin-Tin spheres must be larger than the radii of the atoms they surround. If they are small, potential leaks from atoms can occur. Therefore, inaccurate results may occur in the calculations performed. In this study, the radii of Muffin-Tin

spheres surrounding Nb, Tc, Al, and F atoms were selected as 2.00 a.u., 1.88 a.u., 2.22 a.u., and 2.02 a.u., respectively. Electron convergence values were chosen as 0.0001 e within 1728 special k-points in the first Brillouin zone.

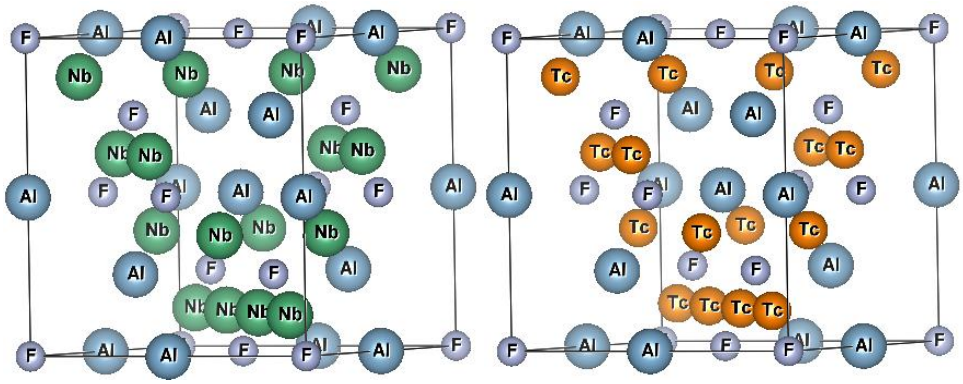

Figure 1. *The molecular schematic representations of $NbAl_2F_4$ and $TcAl_2F_4$ spinels*

3. RESULTS AND DISCUSSION

The energies obtained around the values corresponding to -10%, 8%, 6%, 4%, 2%, 0%, 2%, 4%, 6%, 8% and 10% changes of the lattice parameters, and volume-energy curves of $NbAl_2F_4$ and $TcAl_2F_4$ spinels were obtained. According to these curves, ferromagnetic phases were obtained as more stable for both spinels. Since Murnaghan's equation of state (1944) fit these energy values, the initial state values were calculated, and optimization curves were given in Figure 2.

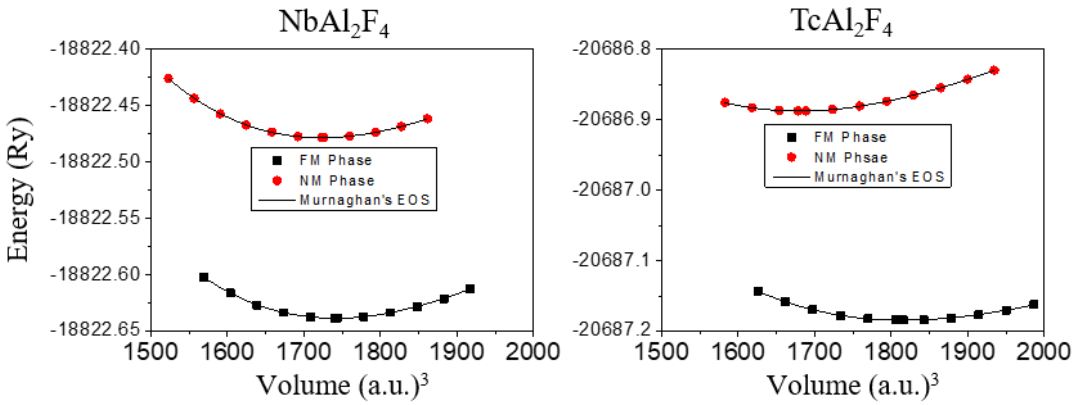

Figure 2. *The calculated energy-volume curves of $NbAl_2F_4$ and $TcAl_2F_4$ spinels*

Equilibrium lattice parameters, bulk modulus and the first derivative of bulk modulus, equilibrium volume and energy values of $NbAl_2F_4$ and $TcAl_2F_4$ spinels were given in Table 1. The lattice parameter of $NbAl_2F_4$ spinel was calculated as 10.11 Å, while it was calculated as 10.25 Å for $TcAl_2F_4$ spinel. The lattice parameter obtained at the equilibrium point of the $TcAl_2F_4$ spinel formed by using the Tc element, whose atomic radius is smaller than the Nb element, is larger. Therefore, the equilibrium lattice parameters of the compounds may need to be evaluated independently of the atomic radii of the elements. Similar studies were obtained by Mahmood et al. (2022). The equilibrium lattice parameters of $CaTi_2S_4$, CaV_2S_4, $CaCr_2S_4$, and $CaFe_2S_4$ spinels obtained as 10.73 Å, 10.75 Å, 10.91 Å, and 10.88 Å when Ti, V, Cr, and Fe elements were used, respectively. Although the atomic radii of the transition metals are used to decrease, the equilibrium lattice parameters and thus the volumes of the compounds obtained tend to increase. However, it may not be right to talk about the fact that this increase or decrease can occur at certain rates. As can be seen, there was a decrease in the lattice parameter when the transition metal Fe was used. The bulk modulus of $NbAl_2F_4$ and $TcAl_2F_4$ spinels were obtained as 51.25 GPa and 48.44 GPa, respectively. Therefore, the resistance of $NbAl_2F_4$ spinel to volume change was higher than that of $TcAl_2F_4$ spinel. The B' value, which shows the value of the bulk modulus against pressure change, was obtained as 4.90 in $NbAl_2F_4$ spinel, while it was obtained as 5.26 in $TcAl_2F_4$ spinel. This is the

expected result. Since the value of the bulk modulus is lower in $TcAl_2F_4$ compound, it indicates that there is a possibility of undergoing more volume changes with the applied pressure. Comparison of decreasing bulk modulus with increasing lattice parameter can be done with $CaTi_2S_4$, CaV_2S_4, $CaCr_2S_4$, and $CaFe_2S_4$ spinels. When Ti, V, Cr, and Fe transition metals were used, the ballast modulus of the structure obtained was 65.38 GPa, 62.10 GPa, 50.00 GPa, and 54.71 GPa, respectively. As can be seen, when Ti, V, and Cr transition metals are used, decreases in bulk modulus were observed inversely with increasing lattice parameters.

Table 1. *The initial state values of $NbAl_2F_4$ and $TcAl_2F_4$ spinels*

Compounds	a (Å)	B (GPa)	B'	V_0 (a.u.)^3	E_0 (Ry)
$NbAl_2F_4$	10.11	51.25	4.90	1740.807	-18822.638
$TcAl_2F_4$	10.25	48.44	5.26	1815.716	-20687.184

After the obtained initial state values, the electronic properties of $NbAl_2F_4$ and $TcAl_2F_4$ spinels were investigated. First, the total densities of states (TDOS) were plotted for the -10 eV and +8 eV energy regions and were given in Figure 3.

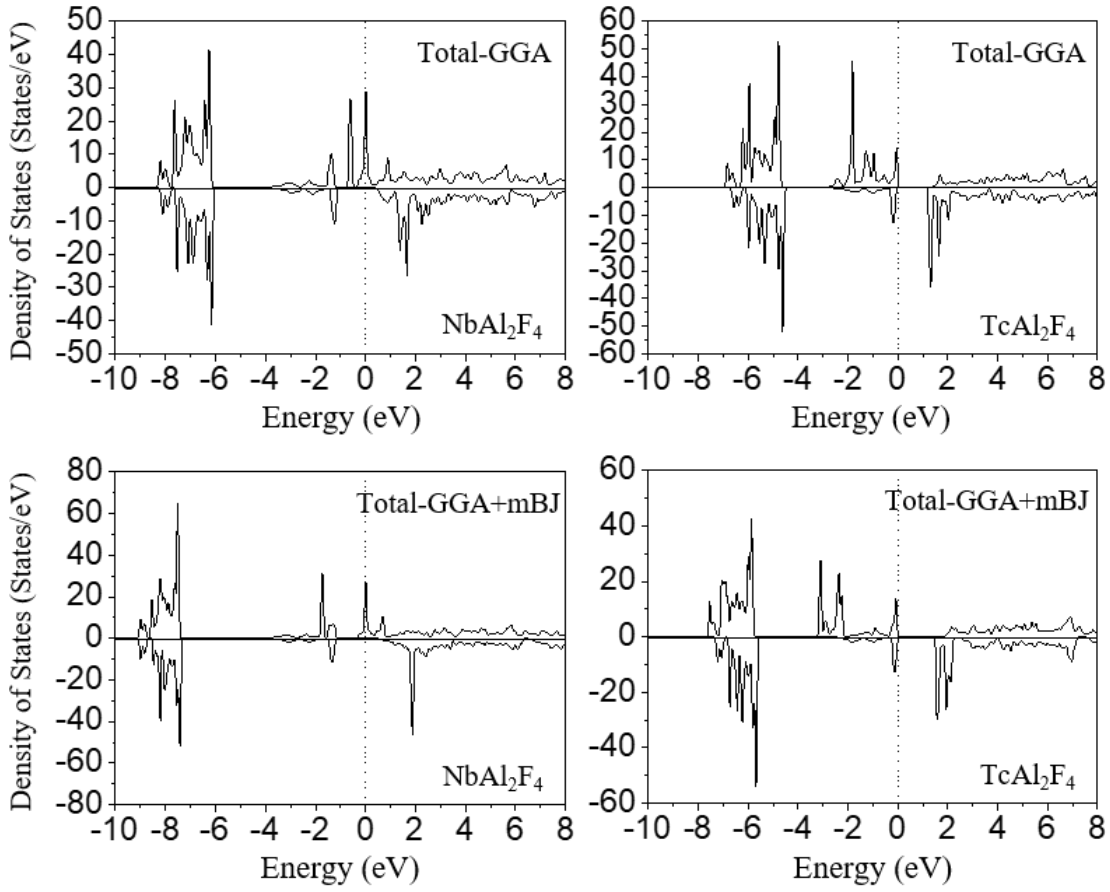

Figure 3. *TDOS of $NbAl_2F_4$ and $TcAl_2F_4$ spinels*

Positive values of the total densities of states represented up-spins (majority), while negative values represent down-spins (minority). In the far negative energy densities of $NbAl_2F_4$ spinel, sharp peaks were observed at the GGA method. The 100% symmetry between the up and down spins indicated that electrons were bounded in these energy regions. These conditions were the same both in the value obtained by the GGA+mBJ of $NbAl_2F_4$ spinel and in the calculation results of $TcAl_2F_4$ spinel. The vertical dotted lines at total densities of states indicated Fermi energy levels. As the Fermi energy levels were approached, there were separations in the electron densities. At each method, the up-spin electrons of $NbAl_2F_4$ spinel contacted Fermi energy levels. This showed that the valence electrons can pass to the conduction band, that is, the metallic character revealed.

In down-spins, band gaps existed. In down-spin states, $NbAl_2F_4$ spinel had a semiconductor character. Therefore, $NbAl_2F_4$ spinel was a half-metallic ferromagnetic material. It is possible to see band gaps in both the up and down spins of $TcAl_2F_4$ spinel when using the GGA and GGA+mBJ. In this case, $TcAl_2F_4$ spinel had a semiconducting nature. The differences in the symmetry between the up and down spins of $NbAl_2F_4$ spinel around the Fermi energy level allow for the formation of a net magnetic character. Likewise, the presence of these asymmetric electron distributions in energy ranges near the Fermi energy level of $TcAl_2F_4$ spinel made the magnetic characters appear. It is possible to talk about studies similar to the electronic structure of spinels in this study. Nazar et al. (2022) investigated the magnetic and electronic calculations of Gd_2MgS_4 and Tm_2MgS_4 spinel sulfides using the first principles method. The band gaps of the up and down electrons of the Gd_2MgS_4 spinel were obtained as 1.44 eV and 1.65 eV, respectively. Thus, Gd_2MgS_4 spinel showed a semiconductor character. While the up spins of the Tm_2MgS_4 spinel showed a metallic character, the down spins showed a semiconductor character. Therefore, Tm_2MgS_4 spinel was obtained as half-metallic ferromagnetic by Nazar et al. (2022). The electronic properties of the semiconductor and half-metallic spinels Gd_2MgS_4 and Tm_2MgS_4 obtained by Nazar et al. (2022) show similar characteristics to the electronic properties of $TcAl_2F_4$ and $NbAl_2F_4$ spinels obtained in this study.

The atomic contributions of $NbAl_2F_4$ and $TcAl_2F_4$ spinels were shown in Figure 4 and Figure 5 to investigate the partial electron densities to the total electron distributions. The electron contributions of the 4d transition metals Nb and Tc atoms were shown in the energy range of -6 eV to +6 eV. Their changes clearly and unequivocally come from these transition metals. Nb atoms have band gaps in their down-spins while their up-spin cuts the Fermi energy levels. This supports TDOS. Most electron contributions come from d-orbitals in transition metals. In the -9 eV and -6 eV energy regions, contributions belong to the p-orbitals of fluorine atoms, while the main contributions come from the s-orbitals of aluminum atoms. This is the expected result because Nb atom has 5 electrons in 4d orbital, Tc atom has 4 electrons in 4d orbital and 1 electron in 5s orbital. The main electron contributions of 4d orbitals of Nb and Tc atoms have also been shown by Saberi et al. (2014) in transition metals doped to GaN nanotubes, Zhang et al. (2022) in Tc, Ru, Rh, and Cd doped to the blue P monolayer, Ali et al. (2021) in K_2NbCl_6 and Rb_2NbCl_6 variant perovskite compounds. In short, the electronic properties obtained in this study gave similar results with many studies in the literature.

It can be said that the electron distributions of aluminum and fluorine atoms of both $NbAl_2F_4$ and $TcAl_2F_4$ spinels have almost 100% symmetry. That is, the electrons of the aluminum and fluorine atoms are almost completely bounded. Both total and partial electron (PDOS) states show that $NbAl_2F_4$ spinel shows a half-metallic character, while $TcAl_2F_4$ spinel shows a semiconductor character.

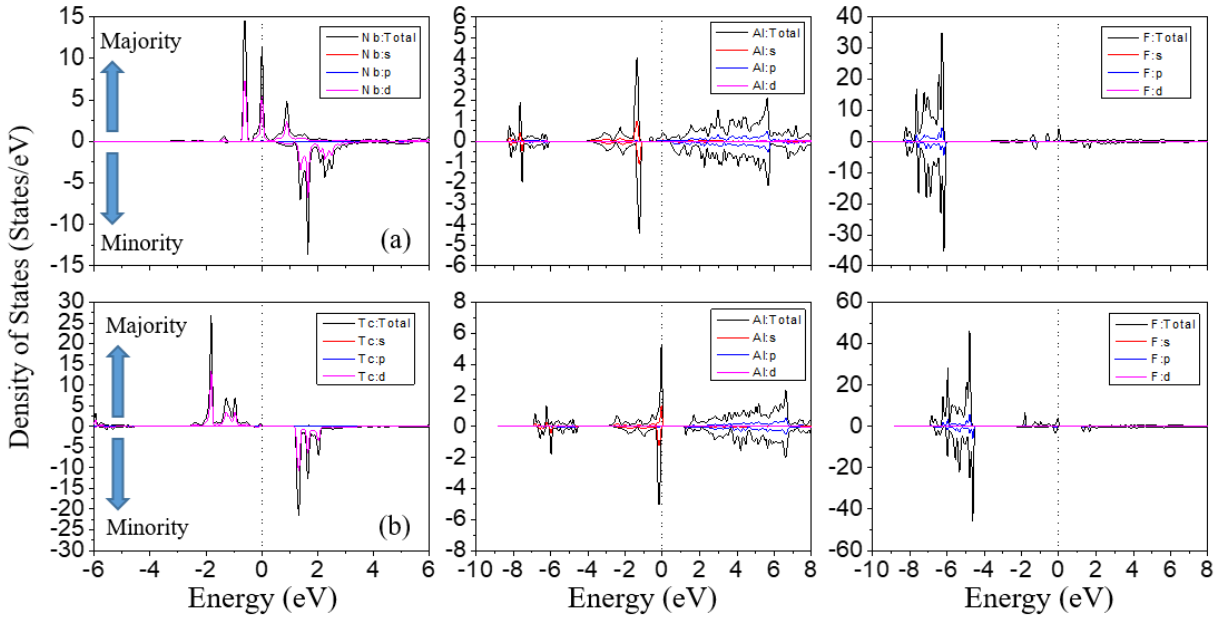

Figure 4. *The obtained PDOS of (a) $NbAl_2F_4$ and (b) $TcAl_2F_4$ spinels in GGA method*

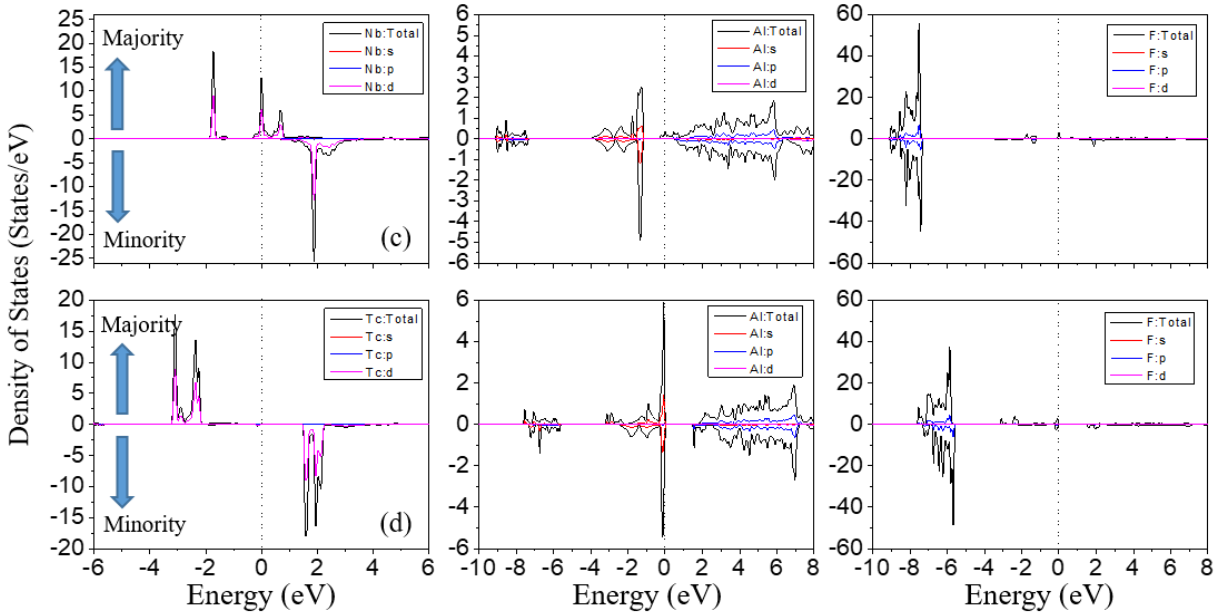

Figure 5. *The obtained PDOS of (c)$NbAl_2F_4$ and (d) $TcAl_2F_4$ spinels in GGA+mBJ method*

In order to support all these densities of states, the band structures were obtained and given in Figure 6 for the up and down spins of $NbAl_2F_4$ and $TcAl_2F_4$ spinels. It can be clearly seen in Figure 6 that the up-spins of $NbAl_2F_4$ spinel show metallic character by cutting the Fermi energy levels in each method. In the GGA, electron densities are available in the -0.5 eV energy region. However, in the GGA+mBJ, all the electrons are destroyed in the range of 0 to -1 eV. Electron densities obtained in the GGA shifted to the range of -2 eV in the GGA+mBJ. In other words, the GGA+mBJ directly affected the energy gaps of the valence electrons.

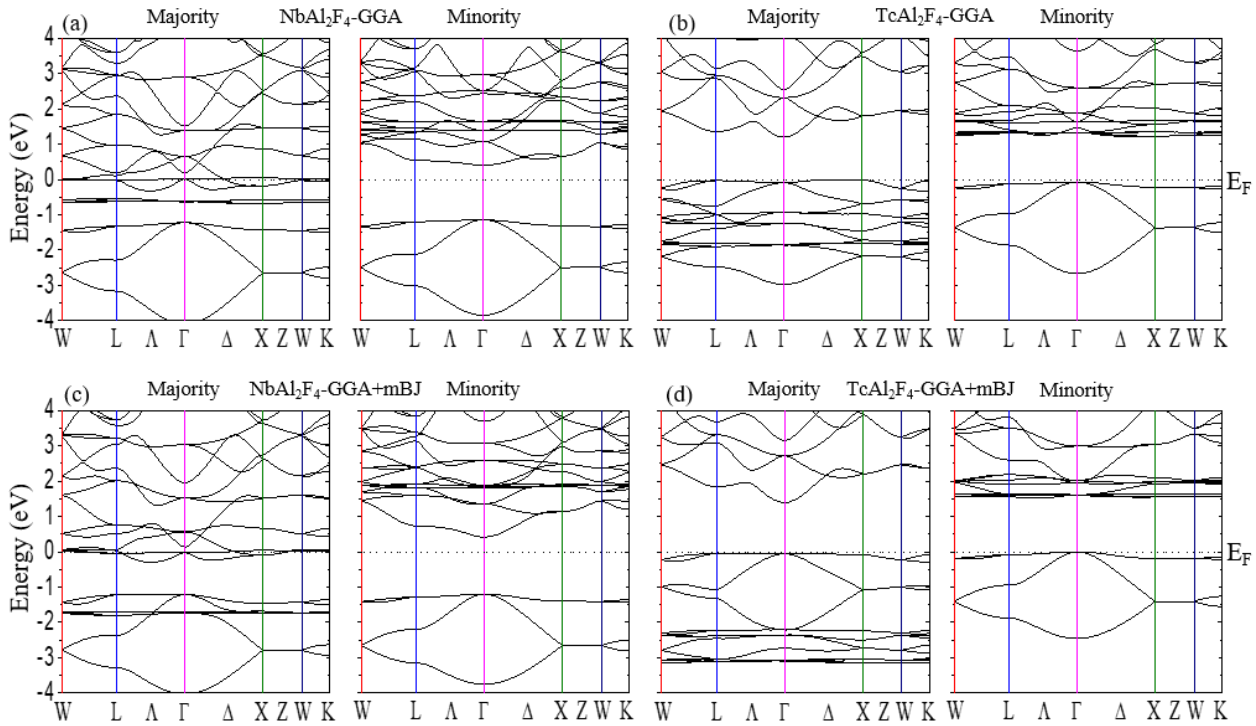

Figure 6. *The calculated majority (up-spin) and minority (down-spin) band structures of $NbAl_2F_4$ and $TcAl_2F_4$ spinels*

In down-spin states, there are direct band gaps in each method. Valence band maximum (VBM) and conduction band minimum (CBM) values were at Γ-points. VBM, CBM, band gap (E_g) and HM band gap (E_{HM}) values of $NbAl_2F_4$ and $TcAl_2F_4$ spinels were given in Table 2 and Table 3 for each method.

Table 2. *The calculated VBM, CBM, E_g and E_{HM} of down-spin of $NbAl_2F_4$ spinel*

Compounds	VBM (eV)	CBM (eV)	E_g (eV)	E_{HM} (eV)
$NbAl_2F_4^{GGA}$	-1.141	0.410	1.551	0.410
$NbAl_2F_4^{GGA+mBJ}$	-1.200	0.422	1.622	0.422

Table 3. *The calculated VBM, CBM, and E_g of both up and down-spins of $TcAl_2F_4$ spinel*

Compounds	$VBM^{Majority}$ (eV)	$CBM^{Majority}$ (eV)	$VBM^{Minority}$ (eV)	$CBM^{Minority}$ (eV)	$E_g^{Majority}$ (eV)	$E_g^{Minority}$ (eV)
$TcAl_2F_4^{GGA}$	0	1.199	-0.067	1.214	1.199	1.281
$TcAl_2F_4^{GGA+mBJ}$	-0.047	1.400	0	1.519	1.447	1.519

In GGA calculations, the VBM and CBM values were calculated as -1.414 eV and 0.410 eV, respectively. In the GGA+mBJ, the VBM and CBM values were -1.200 eV and 0.422 eV, respectively. According to these results, the band gap values were obtained 1.551 eV and 1.622 eV in GGA and GGA+mBJ, respectively. The band gap values in the down spins of $NbAl_2F_4$ spinel, a HM ferromagnetic material, can be calculated as different values in different applied methods. The band gaps of both the up and down spins of $TcAl_2F_4$ spinel with semiconductor character can be clearly seen. There are direct band gaps in each method. In Figure 6, the band gaps increase when the GGA+mBJ is used. In addition, the VBM values in the up-spins are 0 and -0.047 eV in the GGA and GGA+mBJ, respectively, while the CBM values are 1.199 eV and 1.400 eV, respectively. Therefore, band gaps in the up-spin of $TcAl_2F_4$ spinel were obtained as 1.199 eV and 1.447 eV in GGA and GGA+mBJ, respectively. When using the GGA method in down-spin conditions, the VBM value was calculated as -0.067 eV, while the CBM value was obtained as 1.214 eV. The band gap in the down-spin of the $NbAl_2F_4$ spinel using the GGA method was 1.281 eV. When the GGA+mBJ was used, it was observed that the valence band electrons approached the Fermi energy level. The CBM value was 1.519 eV while the VBM value was 0. In other words, the E_g was obtained as 1.519 eV in the GGA+mBJ. The E_g values obtained in GGA+mBJ methods increased in both spinels. In short, while $NbAl_2F_4$ spinel is a HM ferromagnetic material with its semiconductor character in its down-spins, $TcAl_2F_4$ spinel was obtained as a semiconductor ferromagnetic material with its semiconductor character in both up and down spins.

Total magnetic moment values of $NbAl_2F_4$ and $TcAl_2F_4$ spinels were obtained as 6.00 μ_B/cell and 10.0 μ_B/cell, respectively. Most contributions to the total magnetic moments came from the Nb and Tc transition metals. The partial magnetic moments of the $NbAl_2F_4$ spinel are 1.561 μ_B/f.u., 0.003 μ_B/f.u. and 0.031 μ_B/f.u. for Nb, Al and F, respectively. The partial magnetic moments of $TcAl_2F_4$ spinel are 3.149 μ_B/f.u., 0.003 μ_B/f.u. and 0.092 μ_B/f.u. for Tc, Al and F, respectively. It was mentioned that the unbounded electrons at the total state densities are the 4d transition metals Nb and Tc. Therefore, these unbounded electrons did not create magnetic moments. It is clearly seen how much these electron contributions in Fermi energy levels affect the magnetic moments. As a result, $NbAl_2F_4$ spinel is a HM ferromagnetic material with 6.00 μ_B/cell magnetic moment, while $TcAl_2F_4$ spinel is a semiconductor ferromagnetic material with 10.0 μ_B/cell magnetic moment.

4. CONCLUSION

In this study, the electronic and magnetic properties of $NbAl_2F_4$ and $TcAl_2F_4$ spinels were investigated. Ferromagnetic phases of spinels were found to be more stable at ground state values. $NbAl_2F_4$ spinel was obtained as a true half-metallic ferromagnetic in each method. In the down-spins of $NbAl_2F_4$ spinel, the E_g=1.551 eV and E_g=1.622 eV values were found for the GGA and GGA+mBJ, respectively. However, since the value of electron densities closest to the Fermi energy level was CBM, the half-metallic band gaps were obtained as E_{HM}=0.410 eV and E_{HM}=0.422 eV in each method. $TcAl_2F_4$ spinel showed semiconductor character

in both methods. The band gaps in the up-spins were obtained as E_g=1.199 eV and E_g=1.447 eV, respectively, while the band gaps in the down-spins were obtained as E_g=1.281 eV and E_g=1.519 eV, respectively. $NbAl_2F_4$ and $TcAl_2F_4$ spinels have high magnetic moment values. The magnetic moment of $NbAl_2F_4$ spinel was obtained as 6.00 μ_B/cell, while it is 10.0 μ_B/cell in $TcAl_2F_4$ spinel. In both spinels, the most contributions belonged to the 4d transition metals Nb and Tc. As a result, $NbAl_2F_4$ spinel is a true half-metallic ferromagnetic and $TcAl_2F_4$ spinel is obtained as a semiconductor ferromagnetic material, and they are good alternative materials in spintronic applications for experimental works.

CONFLICT OF INTEREST

The author declares no conflict of interest.

REFERENCES

Ali, M. A., Ullah, R., Abdullah, S., Khan, M. A., Murtaza, G., Laref, A., & Kattan, N. A. (2021). An investigation of half-metallic variant perovskites A_2NbCl_6 (A= K, Rb) for spintronic based applications. *Journal of Solid State Chemistry*, *293*, 121823. doi:10.1016/j.jssc.2020.121823

Birsan, A., & Kuncser, V. (2022). Half-metallic properties of Zr_2CrAl ferrimagnetic full-Heusler compound, investigated in tetragonal, orthorhombic and rhombohedral crystal structures. *Journal of Alloys and Compounds*, *900*, 163491. doi:10.1016/j.jallcom.2021.163491

Blaha, P., Schwarz, K., Tran, F., Laskowski, R., Madsen, G. H. K., & Marks, L. D. (2020). WIEN2k: an APW+lo program for calculating the properties of solids. *The Journal of Chemical Physics*, *152*, 074101. doi:10.1063/1.5143061

Blaha, P., Schwarz, K., Madsen, G. K. H., Kvasnicka, D., Luitz, J., Laskowski, R., Tran, F., & Marks, L. D. (2022) *WIEN2k An Augmented Plane Wave Local Orbitals Program for Calculating Crystal Properties*. Vienna University of Technology Institute of Materials Chemistry, Vienna, Austria. ISBN 3-9501031-1-2 PDF

Bouhbou, M., Moubah, R., Bakkari, K., Zaari, H., Sabrallah, A., Khelfaoui, F., Mliki, N., Abid, M., Belayachi, A., & Lassri, H. (2019). Magnetic, half-metallicity and electronic studies of $Cd_{1-x}Zn_xCr_2Se_4$ chromium selenospinels. *Journal of Magnetism and Magnetic Materials*, *476*, 86-91. doi:10.1016/j.jmmm.2018.12.063

de Groot, R. A., Mueller, F. M., van Engen, P. G., & Buschow, K. H. J. (1983). New class of materials: half-metallic ferromagnets. *Physical Review Letters*, *50*(25), 2024-2027. doi:10.1103/PhysRevLett.50.2024

Hirohata, A., Yamada, K., Nakatani, Y., Prejbeanu, I.-L., Diény, B., Pirro, P., & Hillebrands, B. (2020). Review on spintronics: Principles and device applications. *Journal of Magnetism and Magnetic Materials*, *509*, 166711. doi:10.1016/j.jmmm.2020.166711

Khanal, P., Zhou, B., Andrade, M., Mastrangelo, C., Habiboglu, A., Enriquez, A., Fox, D., Warrilow, K., & Wang, W.-G. (2022). Enhanced magnetoresistance in perpendicular magnetic tunneling junctions with $MgAl_2O_4$ barrier. *Journal of Magnetism and Magnetic Materials*, *563*, 169914. doi:10.1016/j.jmmm.2022.169914

Mahmood, Q., Nazir, G., Alzahrani, J., Kattan, N. A., Al-Qaisi, S., Albalawi, H., Mera, A., Mersal, G. A. M., Ibrahim, M. M., & Amin, M. A. (2022). Room temperature ferromagnetism and thermoelectric behavior of calcium based spinel chalcogenides CaZ_2S_4 (Z= Ti, V, Cr, Fe) for spintronic applications. *Journal of Physics and Chemistry of Solids*, *167*, 110742. doi:10.1016/j.jpcs.2022.110742

Murnaghan, F. D. (1944). The Compressibility of Media under Extreme Pressure. *Proceedings of the National Academy of Sciences*, *30*(9) 244-247. doi:10.1073/pnas.30.9.244

Nadeem, A., Bashir, A. I, Azam, S., Rahman, A. U., & Iqbal, M. A. (2022). First-principles quantum analysis on the role of V-doping on the tuning of electronic and optical properties of spinel oxides $MnTi_2O_4$. *Materials Science & Engineering B*, *278*, 115643. doi:10.1016/j.mseb.2022.115643

Nazar, M., Nasarullah, Aldaghfag, S. A., Yaseen, M., Ishfaq, M., Khera, R. A., Noreen, S., & Abdellattif, M. H. (2022). First-principles calculations to investigate structural, magnetic, optical, electronic and

thermoelectric properties of X_2MgS_4 (X= Gd, Tm) spinel sulfides. *Journal of Physics and Chemistry of Solids*, *166*, 110719. doi:10.1016/j.jpcs.2022.110719

Patel, P. D., Pandya, J., Shinde, S., Gupta, S. D., & Jha, P. K. (2022). Robust half metallic ferrimagnetic behavior and thermoelectric response of newly discovered Full-Heusler compound Mn_2SiRh: DFT study. *Materials Today: Proceedings*, *67*(6), 939-942. doi:10.1016/j.matpr.2022.07.468

Perdew, J. P., Burke, K., & Ernzerhof, M. (1996). Generalized Gradient Approximation Made Simple. *Physical Review Letters*, *77*, 3865. doi:10.1103/PhysRevLett.77.3865

Quiroz, H. P., Calderón, J. A., & Dussan, A. (2020). Magnetic switching control in Co/TiO_2 bilayer and TiO_2:Co thin films for Magnetic-Resistive Random Access Memories (M-RRAM). *Journal of Alloys and Compounds*, *840*, 155674. doi:10.1016/j.jallcom.2020.155674

Rafiq, M. A., Javed, A., Rasul, M. N., Nadeem, M., Iqbal, F., & Hussain, A. (2022). Structural, electronic, magnetic and optical properties of AB_2O_4 (A = Ge, Co and B = Ga, Co) spinel oxides. *Materials Chemistry and Physic*s, *257*, 123794. doi:10.1016/j.matchemphys.2020.123794

Ravi, S. (2020). Spin transport through silicon using a double perovskite-based magnetic tunnel junction. *Superlattices and Microstructures*, *147*, 106688. doi:10.1016/j.spmi.2020.106688

Saberi, S. H., Baizaee, S. M., & Kahnouji, H. (2014). Electronic structure and magnetic properties of transition-metal (Y, Zr, Nb, Mo, Tc, Ru, Rh, Pd, Ag and Cd) doped in GaN nanotubes. *Superlattices and Microstructures*, *74*, 52-60. doi:10.1016/j.spmi.2014.05.013

Shin, B., Park, I. H., & Chung, C. W. (2006). Inductively coupled plasma reactive ion etching of Co_2MnSi magnetic films for magnetic random access memory. *Studies in Surface Science and Catalysis*, *159*, 377-380. doi:10.1016/S0167-2991(06)81612-5

Singh, D. J. (1994). *Planewaves, Pseudopotentials and the LAPW Method*. Kluwer Academic, Boston. doi:10.1007/978-1-4757-2312-0

Tran, F., & Blaha, P. (2009). Accurate band gaps of semiconductors and insulators with a semi-local exchange-correlation potential. *Physical Review Letters*, *102*(22), 226401. doi:10.1103/PhysRevLett.102.226401

Xu, M., Zhang, Q., Tan, Q., Zhang, W., Sang, S., Yang, K., & Ge, Y. (2022). A magnetostrictive $BaTiO_3$-Fe-Ga&PDMS magnetic field sensor: Research on magnetic detection performance. *Sensors and Actuators: A. Physical*, *335*, 113383. doi:10.1016/j.sna.2022.113383

Zhang, J.-M., Duan, J.-P., Huang, Y.-H., & Wei, X.-M. (2022). Effects of the Tc, Ru, Rh and Cd substitution doping on the structural, electronic, magnetic and optical properties of blue P monolayer. *Thin Solid Films*, *756*, 139386. doi:10.1016/j.tsf.2022.139386

Zhang, Z., Sang, L., Huang, J., Chen, W., Wang, L., Takahashi, Y., Mitani, S., Koide, Y., Koizumi, S., & Liao, M. (2020). Enhanced magnetic sensing performance of diamond MEMS magnetic sensor with boron-doped FeGa film. *Carbon*, *170*, 294-301. doi:10.1016/j.carbon.2020.08.049